ISSS Journal of Micro and Smart Systems (2022) 11:147–167
https://doi.org/10.1007/s41683-022-00092-x

ORIGINAL ARTICLE

Photonic crystal based biosensors: an overview

D. Gowdhami[1] · V. R. Balaji[1] · M. Murugan[2] · S. Robinson[3] · Gopalkrishna Hegde[4]

Received: 15 September 2021 / Revised: 3 December 2021 / Accepted: 5 January 2022 / Published online: 24 January 2022

Abstract
Photonic Crystals (PC) have emerged as interesting photonic structures for the past few decades and play a vital role in the field of optical communication, biomedical sensing, and other applications. Photonic crystals have a major impact in designing the variety of photonic sensors due to its compactness, high sensitivity, high selectivity, fast responsiveness, immunity to electromagnetic noise, etc. The physical property of the photonic crystals is altered to create the sensors for various applications such as temperature, pressure, stress, gas, chemical, biomaterials, etc. PC-based biosensors assure fast response, high accuracy, good quality factor with low losses. Several sensing schemes such as, Surface plasmon resonance, Infra-Red (IR) absorption, Refractive index sensing, and Displacement sensing are used and being explored using different PC design structures. The Effective Refractive Index sensing is the most common sensing mechanism used in Biosensor and optical properties of the sensors are analyzed by comparing the spectral properties of the transmitted and reflected power. This review article aims to discuss about the recent developments in PC-based biosensors with different design structures, analysis, and different analytes, biomaterials. Further, the comparison of the design, structural and performance parameters of various biosensors are tabulated.

Keywords Photonic crystal structure · Photonic band gap · Plane wave expansion · Finite Difference Time Domine · Analyte · Biosensors

Introduction

The field of Photonic Crystal (PC) came into existence in the year 1987 through the great Physicist Yablonovitch (Yablonovitch 1987) and the term Photonic Crystal was given by both Eli Yablonovitch and Sajeev John together (John 1987). The Photonic structures designed with periodic dielectric element microstructure or nanostructure with repeating regions of high and low dielectric constants that affect the light wave to propagate through the structure depending upon the wavelength.

Photonic crystal structure can be made periodic either in one (1D), two (2D) or three dimensions (3D). The 1D crystal structure are simple which is used as bio-sensor in diagnosis of malaria and used in designing optical mirrors and they also possess an incomplete bandgap, 3D crystal structures are complex as they have a very small lattice and difficult to use them and 2D structure is widely used as it possesses the high confinement of light, ease of fabrication and easily control the propagation modes.

The 2D Photonic Crystal structures are broadly classified into two types 1. Dielectric rods placed in air medium 2. Air holes in dielectric slab. Among these dielectric rods structure placed in air is widely used in many designs as they possess low optical losses (Kok et al. 2009). The lattice arrangement of the Photonic crystals may be fully periodic, quasi-periodic, and non-periodic in nature. Depending upon the design of the optical device the lattice structure is chosen among which the square and hexagonal lattice are used as it provides easy integration with other

✉ D. Gowdhami
photonics.material@gmail.com

[1] School of Electronics Engineering, Vellore Institute of Technology, Vandalur, Kelambakkam Road, Chennai, Tamil Nadu 600 127, India

[2] Department of Electronics and Communication Engineering, SRM Valliammai Engineering College, Kattankulathur, Tamil Nadu 603203, India

[3] Department of Electronics and Communication Engineering, Mount Zion College of Engineering and Technology, Pudukkottai, Tamil Nadu 622 507, India

[4] Centre for BSSE, Indian Institute of Science, Bengaluru, Karnataka 560012, India

optical devices and wide bandgap in optical frequency range (Joannopoulos et al. 2008).

Due to the periodicity in the material dielectric constant certain bands of wavelength are disallowed in the structure called Photonic Band Gap (PBG), and the electromagnetic waves cannot propagate in PBG (Rajasekar and Robinson 2018a). In 2D PCs, the range of frequencies over which none of the modes are allowed is called PBG. Hence periodicity of the PC has to be broken by including defects. Removing a single lattice point (rods/ holes) in the whole PC structure is called point defects (either called as micro or nanocavity) which allow a particular mode or a group of modes to be propagated in PBG. Further, by removing a row of lattice points is called line defects which again allows a single or a set of modes in the PBG, and these modes cannot be propagated in the rest of the crystal structure and hence it should be an evanescent field. Thus, by introducing point and line defects in the crystal structure the event of spontaneous emission can be controlled (Suzuki and Yu 1999; Joannopoulos et al. 1997). The line defect forms a waveguide, and removing a single rod /hole leads to a cavity defect. Excavating a particular surface in the bulk crystal structure leads to surface defects which allows a state to be localized in one direction(x). Biosensors are designed either with a cavity, waveguide and ring resonator or a combination of the above defects that is based on the designer's requirement.

Photonic crystals (PC) show a very strong confinement of light at very small volume and at nanoscale range the characteristics of the substance are defined. PC sensors have received keen attention among researchers due to its outstanding optical properties such as high sensitivity, high compact sensing unit, quick responsiveness, resistance to electromagnetic interference, and low cost. It is used in wide range of application in industrial and biomedical topics (Nair and Vijaya 2010). The major advantage of PC sensors is that converting a very small amount of analyse into detectable signals which is used in many sensing applications such as Multiplexer, Demultiplexer, Lasers, Fibers, Logic gates, Waveguides, Filters, Optical sensors, etc. With the recent progress in micro-nano fabrication, an optimized design of PC-based sensors within the fabrication limit and packaging tolerance is very important. In this review article we discuss about the recent developments in PC-based biosensors with different designs, structures, analysis for different analytes, biomaterials sensing. Further, a comparison table of the design, structural, and performance parameters of various biosensors reported in recent years is presented.

The remaining part of the paper is segregated into 4 sections as follows. Section 2 discusses the Design consideration of a Photonic crystal sensor. Section 3 emphasis the Sensing and Detecting Mechanism. Section 4 presents a detailed literature review of the existing biosensors which is further categorized based on the structure of the biosensors as waveguide-based biosensor, Cavity coupled waveguide biosensor, and Resonator based Biosensor. Other performance parameters are also discussed in detail with Future Design consideration and Sect. 5 concludes the paper.

Design considerations

A sensor is basically a transducer which is used to convert one form of detectable signal from one domain to another domain. Till now many Domains have been explored by many researches such as Electrical domain (Current, Voltage, etc.), Biochemical domain (Blood components, urine, Glucose, etc.), Magnetic domain (Magnetic field), Radiation domain (Absorption, Radiation, and transmission), Mechanical domain (Force, Stress, Strain, etc.), Thermal domain (Temperature). The Silicon on insulator (SOI) technology in the field of photonic sensors paves way for number of sensing applications as listed above and its performance is measured in terms of Sensitivity, Quality Factor, Transmitting capability, etc.

Mathematical parameters

The key parameters which are used to measure the sensor performance are Quality Factor (Q-factor), Wavelength sensitivity(S), Resolution, and Transmission efficiency.

Among this, the measurement of Quality factor defines the light confinement in the PC cavity and Sensitivity defines the change in refractive index in the PC sensor or how much output of the sensor is varying with minute change in input (Kumar and Suthar 2019).

The Quality factor (Q) is defined as the ratio of obtained resonant wavelength to change in the wavelength at Full Width Half Maximum (FWHM). Q should be high as possible and it is unit-less parameter.

$$Q = \frac{\lambda_O}{\Delta\lambda} \tag{1}$$

where λ_O is wavelength at resonance and $\Delta\lambda$ is the difference of wavelengths obtained at FWHM.

The Sensitivity (S) is the ratio of obtained change in the resonant wavelength due to change in the refractive index. Sensitivity is to be measured in terms of nm/RIU and it should be high as possible.

$$S = \frac{\Delta\lambda}{\Delta n} \tag{2}$$

where $\Delta\lambda$ is change in resonant wavelength and Δn is change in refractive index.

The Resolution characterizes the smallest possible spectral shift that can be accurately measured. Numerically, the resolution (R) is calculated as

$$R = \Delta\lambda = \lambda_r - \lambda_s \tag{3}$$

where λ_r is the resonant wavelength, λ_s is the smallest resonant wavelength shift, and $\Delta\lambda$ is the wavelength difference.

The Detection Limit (DL) is given as the ratio of wavelength resolution R to sensitivity S given as

$$D = \frac{R}{S} \tag{4}$$

For RI sensing the DL should be the smallest sample RI change that can be accurately measured.

The Figure of Merit of a sensor can be defined as the following equation

$$FOM = \frac{(S \times Q)}{\lambda_r} \tag{5}$$

The Transmission efficiency is used to measure the output signal level, which can be calculated by the following equation

$$P = \frac{P_O}{P_I} \tag{6}$$

where P_0 is the output power at the resonance peak and P_I is the input power at the same wavelength.

Sensing schema and detecting mechanism

The Photonic refractive index sensing capabilities are based on the two fundamental techniques such as Homogeneous sensing and Surface (Heterogenous) sensing (Chao et al. 2006). Among this, the Surface sensing method enables specificity and label-free detection as light strongly interacts with the analytes as the photon lifetime is high which provides higher sensitivity and selectivity (Bougriou et al. 2014).

Two detecting schemes are used to transduce the analytes into detectable signals, one is by monitoring the resonant wavelength shift and the other is intensity variation at a selected wavelength. The former schema shows the change in the resonant wavelength corresponds to the Refractive index change of the analytes which leads to higher quality factor and sensitivity with wider wavelength shift and in the later schema, it is simple and accurate but it has a narrow range of wavelength shift (Chao et al. 2006).

Numerical methods

There are many methods in which the dispersion behavior and transmission spectra of the Photonic crystals can be analyzed such as transfer matrix method (TMM), plane wave expansion method (PWE), finite difference time domain method (FDTD), and finite element method (FEM), each has its unique properties. Among these, the FDTD and PWE are predominantly used methods because of their performance to meet the demand to analyze the PC. The PWE method is initially used for the theoretical analysis of the PC structures as the eigenmode in periodic structure can be expressed as a superposition of set of plane waves. In this method the dispersion properties such as photonic bandgap and propagation modes are precise, but the transmission spectra, back reflections, and field distribution cannot be obtained as it considers only the propagating modes which turns to be the limitation of PWE method. Thus, the transmission spectra and the field distribution can be solved numerically with respect to the Maxwell equations using FDTD method. So, PWE method is used to calculate the photonic bandgap and the FDTD method is used to calculate the power spectrum transmission.

Biosensors

In 1962, Clark and Lyons were the first to detect the optical sensing mechanism (Clark and Lyons 1962) and it paved way for a number of optical sensor application. Biosensor is an analytical device which detects a particular analyte such as enzyme, DNA, Pathogens, etc. and converts the biological response into detectable signals. The major elements of biosensor are the biological recognition system to detect the analyte, transducer which converts the biological information into detectable signals, and signal processing unit which processes the signal and displacement in the display unit. The biosensing depends upon the sensing domain. Figure 1 shows the Major elements of Biosensor.

Types of biosensors

They are broadly classified based on the bio transducer type. The most widely used bio transducers are given as: (Naresh and Lee 2021).

- Thermal biosensors
- Acoustic biosensors
- Optical biosensors

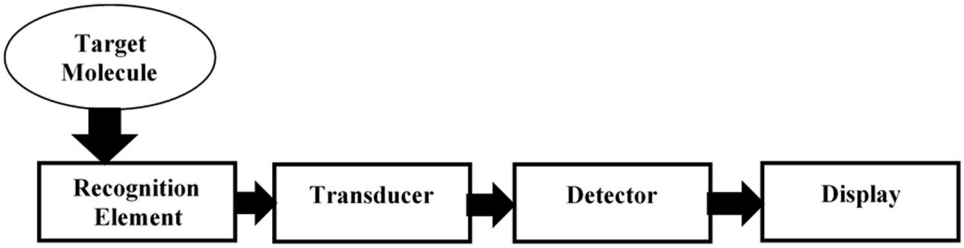

Fig. 1 Major elements of Biosensor

Optical biosensor

An Optical biosensor is an analytical device which is used to convert the target's biological data into optical signal. Maximum it relies on the evanescent field that can be monitored in real-time. As the light interacts with analyse the change in refractive index leads to the variation in intensity or in wavelength shift. Thus, the optical sensors utilize the optical property such as change in refractive index of the analyte to sense the analyte. Fiber Bragg grating (FBG) and Surface plasma resonance are the other sensing technique used so far. PC biosensors also play a major role in optical sensing and there is a great demand for the development of highly sensitive, fast responding, easy to use, and low-cost sensors for the detection of recognition of the analyte. This demand can be fulfilled by the PC-based optical biosensors.

Principal of operation of PC-based biosensor

The Optical biosensor system consists of an Optical source, followed by PC-based Biosensor, Photodetector, Signal processing unit, and Display unit. Figure 2 represents the Schematic of optical sensing system.

There is number of applications for biosensors which are depicted in Fig. 3. It is used in Disease detection, Drug discovery, Soil Quality Monitoring, etc. (Singh et al. 2020).

The photonic crystal sensors use different techniques such as Refractive index sensing, Displacement sensing, Infra-Red (IR) absorption, Surface Plasmon resonance, and Non-linear characteristics of PC. We have other optical devices based on photonic crystals such as optical filters (Robinson and Nakkeeran 2012a; Rajasekar et al. 2019), demultiplexers (Balaji et al. 2016), logic gates (Salmanpour et al. 2015), switches (Tameh et al. 2011), power splitter (Bayindir et al. 2000), channel drop filter (Rajasekar and Robinson 2018b), add-drop filters (Radhouene et al. 2021) and directional couplers (Luff et al. 1996). Sensors has many applications as Temperature sensors

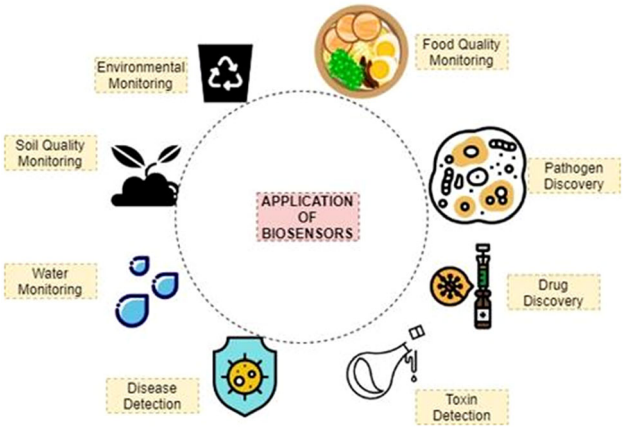

Fig. 3 Applications of biosensors

(Radhouene et al. 2017), Pressure sensors (Bahaddur et al. 2019), Chemical sensors (Painam et al. 2017), Fluid sensor (Patil et al. 2013) and Biosensors (Chow et al. 2004; Kurt and Citrin 2005; Krupa and Triveni 2020; Nischita et al. 2015; Sharma and Sharan 2014a, 2015, 2014b; Sharma et al. 2015; Sundhar et al. 2019; Kulkarni et al. 2020; Painam et al. 2014, 2016; Ameta et al. 2017a, 2017b; Jindal et al. 2016; Harhouz and Hocini 2015; Hocini and Harhouz 2016; Sani et al. 2021; Kumar et al. 2020; Robinson and Dhanlaksmi 2017; Robinson and Nakkeeran 2012b; Chhipa et al. 2017; Arunkumar et al. 2019; Arafa et al. 2017; Areed et al. 2017; Huang et al. 2014; Chopra et al. 2016; Swain and Palai 2016; Suganya and Robinson 2017; Olyaee and Mohebzadeh-Bahabady 2014).

In this paper, an overview of 2D-Photonic crystal structure with respect to various Biosensors is reviewed. In the past few decades Biosensor is a fast-growing area in the field of research as it is involved in label-free affinity-based optical sensors. This is done by measuring the change in the refractive index for sensing the analytes using Photonic crystal structure as it provides the unique light confinement mechanism at micro and nanoscale ranges. A 2D PC biosensor was designed with a microcavity fabricated on a

Fig. 2 Schematic structure of optical sensing system

Silicon on Insulator (SOI) substrate, with sensing area of $\sim 10\mu m^2$, the ambient change in refractive index or resolution as 0.002 (Chow et al. 2004). A photonic crystal waveguide-based biosensor was designed. In this change in refractive index of a DNA sample was observed by changing the radii of air holes in a given row which shifts the resonant frequency and the overall device exhibits a sensitivity enhancement and requires only very small number of analytes of picolitres (Kurt and Citrin 2005).

Different types of PC-based bio-sensors

Photonic Crystal based Optical Biosensors can be broadly classified based on the structure as follows.

1. Waveguide-based Biosensors.
2. Cavity coupled waveguide-based Biosensors.
3. Resonators-based Biosensors.

Waveguide-based biosensors

A waveguide-based sensor can be formed by introducing a line defect in the Photonic crystal. These waveguide PC has been used in detecting biological analytes as they effectively control the light-matter interaction and hence used in sensing applications.

Krupa and Triveni (2020) proposed a biosensor for detection of pregnancy based on Human Chorionic gonodotropin (HGC) in urine. The size of the sensor is about 6 μm×6 μm, Rods in air configuration are used with a square lattice structure operates at 1590 nm to 1600 nm. In this sensor, both line and point defects are used for sensing purpose. Change in RI of urine of pregnant women by the detection of Human Chorionic gonodotropin (HGC) a corresponding change in the output transmission flux is observed for different urine samples. Figure 4 shows the biosensor.

Nischita et al. (2015) projected a biochip for DNA analysis of Breast cancer. A square lattice with line defect and dielectric Si rods in air configuration is used. An analysis of normal cell breast DNA and Breast Cancer cell DNA has been done. The change in ERI is the basic principle used in this sensor. The obtained spectral behavior shows the maximum amplitude for normal breast DNA is 0.1802 whereas for benign DNA and malignant DNA is 0.1791 and 0.1795 respectively. Due to the change in the refractive index of the analyte, the wavelength shifts were observed for normal breast DNA at 1.845 um and benign DNA at 1.846 um, and malignant DNA at 1.8447 um. The sensitivity of the sensor is observed as 10^{-6} with very good quality factor of 118,563.

Sharma and Sharan (2014a) designed a biosensor to detect the Concentration of Glucose in urine. Rods in air configuration with hexagonal symmetry is and a lattice constant of 100 nm is used. Various concentration of the glucose present in the urine (Normal (0–15 mg/dl), 0.625 gm/dl, 1.25 gm/dl, 2.5 gm/dl, 5 gm/dl, and 10 vgm/dl) was sensed and the output resonant frequency varies as there is a change in refractive index of the urine. The sensor is highly sensitive for a small change in the refractive index about 0.001 the resonant frequency changes to 0.00002. It specifically gives a very good output for Hypoglycemia (very low level of Glucose concentration 40–60 mg/dl in blood).

Sharma and Sharan (2015) proposed a biosensor to detect Glycosuria in urine. The Air holes in Si slab configuration with hexagonal lattice structure is used. The lattice constant of 0.1 um and radius of the air holes is 420 nm. Urine samples with different glucose concentration [Normal (0–15 mg/dl), 0.625 gm/dl, 1.25 gm/dl, 2.5 gm/dl, 5 gm/dl, and 10 gm/dl] are taken and for a minute change in refractive index of the urine there is decrease in the normalized output transmission flux with a very good quality factor. In addition, it is also detecting Diabetes mellitus as the urine, refractive index varies as the blood glucose level varies and hence the transmitted output power level varies. Figure 5 depicts the proposed biosensor.

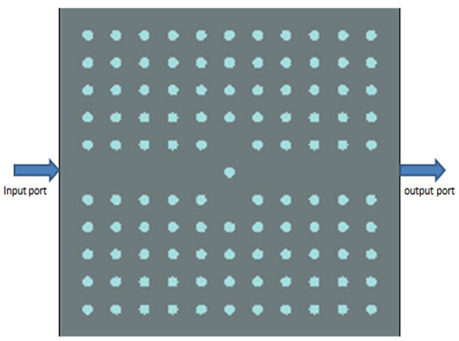

Fig. 4 Design of Bio sensor

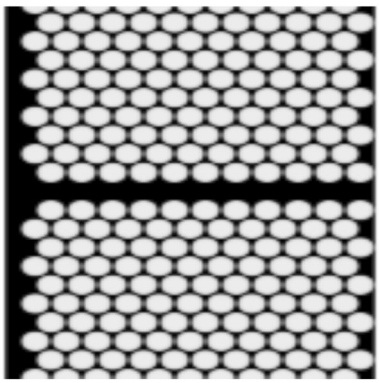

Fig. 5 Image of Biosensor

In the paper by Sharma et al. (2015), a grating-based 2D photonic crystal was designed for the analysis of Basal, Breast, and Cervical cancer cells. In 15 × 20 matrix, grating was incorporated with a line defect. Cubic symmetry with Dielectric Si rods in air with a diameter of 380 nm is incorporated in the sensor. The period of the grating rods is placed at 1um which gives a good sensitivity with the change in refractive index of the normal and cancerous cells the reflection spectrum also varies for each type of cell. Figure 6 represents the biosensor to detect the cancer cell.

Sundhar et al. (2019) proposed a biosensor is designed with 'L' and inverted 'L' waveguides with a sensing hole and it is used to detect the cervical cancer cell. The sensor uses a square lattice with rods in air configuration with a periodicity of 588 nm. The photonic bandgap ranges from 1225 to 1656 nm. By the change in the refractive index of the normal cell and cervical cancer cell the transmission spectrum of the light is shifted to 1650 nm with 100% transmission efficiency and the wavelength of input light is 1550 nm. Figure 7 represents the Sensor of cervical cancer.

Kulkarni et al. (2020) proposed an optical sensor to detect the bacteria (five different types) in the contaminated water. A 2D square grating lattice structure with Rods in air configuration is used with a lattice constant of 1um. A line defect is introduced in the sensor. When the air is replaced by water and light is passed through the sensor, a strong light-matter interaction takes place and the based-on variation of the refractive index of the bacteria(s) the transmission spectrum varies at a selected wavelength of 1550 nm. But the sensor is not selective and sensitive.

Sharma and Sharan (2014b) proposed a sensor to analyze the Normal Lymphocyte cell and its components. A 2D grating-based photonic crystal-based sensor to diagnose the early stage of cancer. The geometry of sensor is given as follows. It has a square lattice structure with a line defect and rods in air bed configuration. The lattice constant is given as 1 μm and the radius of the rods is 0.19 μm. The air is replaced with the sample analyte when the sensor is absorbed by the lymphocyte cells. As the light interacts with the lymphocyte cell and its components the different transmission and reflection spectrum is detected at different

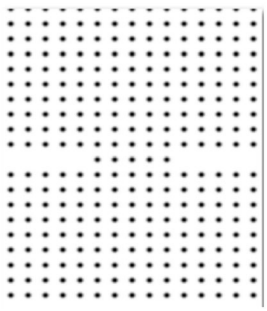

Fig. 6 Design of the Bio sensor

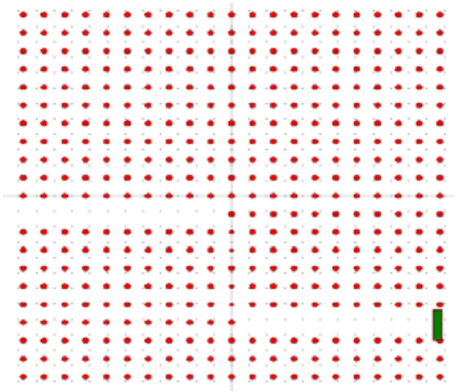

Fig. 7 Biosensor Design

resonant wavelength. The dielectric constant of normal lymphocyte cell varies from 1.8225 to 1.8769 whereas for cancer cell varies from 1.9376 to 1.9628. Thus, refractive indices increase for cancerous cells and FDTD is used for analysis purpose.

Painam et al. (2014) proposed a simple line defect-based Bio-chemical sensor to estimate the concentration of sulphuric acid. The design structure has a photonic crystal waveguide with air holes with a line defect on the silicon wafer. The radius of the air holes is 200 nm with a lattice constant of 1 μm. The variation of electric field intensity with respect to changes in the concentration of sulphuric acid is the basic principle behind the sensor. The operating wavelength of the sensor is 589 nm and with the line defect and without the sample the electric field distribution is 2.20. An air hole is placed in the line defect and is filled with the various concentration of sulphuric acid and its electric field distribution is noted down respectively. The refractive index varies with respect to the concentration and the electric field is obtained as 3.88 V/m, 3.87 V/m, and 3.84 V/m for 90%, 60%, and 30% of Sulphuric acid respectively.

Painam et al. (2016) presented a biosensor structure to detect the pathogen so-called *Escherichia coli* (*E. coli*). An experimental analysis was done to measure its parameters as it was cultured with DH5α strains and its length and diameter ranges from 1.132 to 1.825 μm and 0.447 to 0.66 μm respectively. A Photonic crystal waveguide (PCW) was designed with SiO_2 as the base layer and three active layers such as GaAs (Gallium arsenide), Si (Silicon) or Si_3N_4 (Silicon Nitride) with a thickness of 0.57 μm. The air holes in circular shape with a lattice constant of 1 μm and radius of the air holes as 0.45 μm is used with a hexagonal lattice. A line defect was introduced horizontally at the center of the structure with small cavities with a radius of 0.1 μm and a central bigger cavity of length 1.096 μm and diameter of 0.57 μm.

Plane-wave expansion method is used to obtain the PBG and after the defects are applied $\lambda_1 = 2.55$ µm, $\lambda_2 = 2.6$ µm, and $\lambda_3 = 2.44$ µm are able to propagate through the $GaAs/SiO_2$, Si/SiO_2, and Si_3N_4/SiO_2 PCW. As the *E. coli* (n = 1.39) is trapped in the center of the sensor and when light is passed through the input the resonant shift for $GaAs/SiO_2$, Si/SiO_2 and Si_3N_4/SiO_2 is observed as 1×10^{-4} µm, 6×10^{-4} µm, and 6.06×10^{-8} µm respectively. Si/SiO_2 is observed with the highest sensitivity of 10.10438 nm/RIU but as refractive index changes the sensitivity decrease to 6.73 nm/RIU, $GaAs/SiO_2$ has a medium sensitivity of 2.02 nm/RIU and Si_3N_4/SiO_2 has a very low average sensitivity. Thus, $GaAs/SiO_2$ is preferred to detect *E. coli* as it has a moderate sensitivity. The below Figs. 8a and 8b depict the scanning electron microscopy (SEM) of *E. coli* strain and Biosensor (PCW).

Cavity coupled waveguide-based biosensors

These sensors are constructed by including both the point defect (cavity) and the line defect (waveguide). The cavity can be either microcavity, and nanocavity depending upon the designer's requirement and the sensing analyte. The cavity waveguide structures provide a very good light-matter interaction with the analytes and hence provide a longer photon life-time within the cavity. Thus, it is said to be a very good sensing platform for Biosensors.

Ameta et al. (2017a) A nano-cavity coupled waveguide biosensor is proposed by this author through which different blood components such as cytop, Blood plasma, etc. are detected for a minute change in RI of the analyze there exist a noticeable resonance shift in the transmission spectra. A hexagonal symmetry with rods in air configuration was introduced so that the overall area of the sensor is about 19X15µm^2. The lattice constant of 690 nm and the radius of 220 nm is used. The photonic bandgap was obtained by the plane wave expansion method and the FDTD is used for analysis purpose. To create a nanocavity the radius of the center hole is modified from 220 to 130 nm. When the sensor is dipped into the analyte the transmission output varies according to the change in the refractive index of the blood component. Figure 9 depicts the Design of Biosensor.

Ameta et al. (2017b) designed a multichannel-based nano-cavity coupled biosensor was designed to overcome the limitation of single-purpose sensor. Hexagonal lattice with Si Dielectric Rods is placed over the wafer of air. With the consideration, that different concentration of glucose level in the blood will have different refractive indices a four-channel biosensor was proposed by incorporating drop waveguides and nano cavities. The radius of the Si rods are modified from 200 to 170 nm for the central nanocavities along the four waveguides. Figure 10 represents the Biosensor with four different channels. Four different refractive index is filled in four waveguides and when the analytes are introduced in the sensor the glucose concentration in the blood with 0 mg/dl, 50 mg/dl, 100 mg/dl, and 150 mg/dl was analyzed. The transmission spectra varies according to the change in refractive index of the glucose concentration. The operating wavelength varies from 1300 to 1700 nm and the input wavelength is 1550 nm.

Jindal et al. (2016) proposed a nanocavity coupled photonic crystal waveguide which is used to sense five different cancer cells with high-Quality factor, selectivity and sensitivity. The Effective change in the refractive index is the principle used in the biosensor as cancer cells exhibit larger RI than normal cells and the nucleus contains large amount of protein for cell division. The cancer cells such as Jurkat, HeLa, PC-12, MDA-MB-231, and MCF-7 are analyzed in this biosensor. A Hexagonal lattice structure with silicon rods in air configuration is considered for design purpose with a lattice constant of a = 0.8um and the radius of the Si rods as 0.3a. Plane Wave Expansion (PWE) method is used to calculate the transmission spectra for TE Photonic Band Gap (PBG) for normalized frequency of

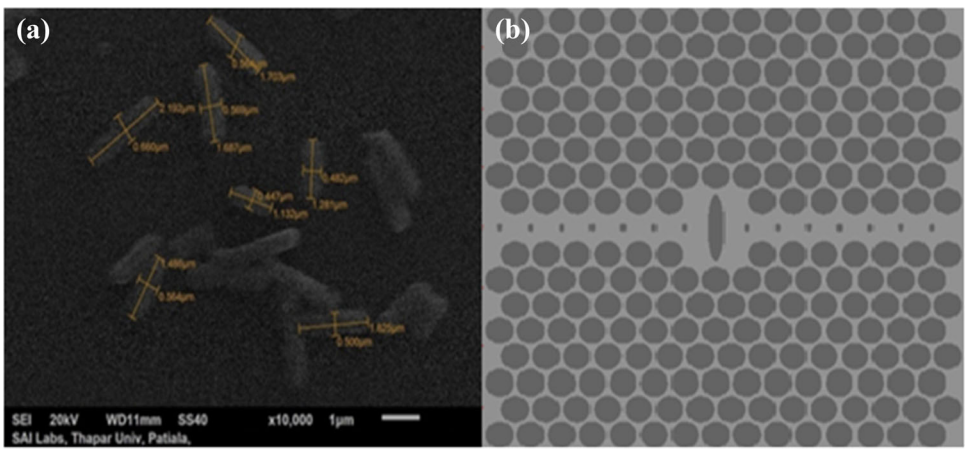

Fig. 8 **a** SEM image of E. coli strain. **b** line with point defect in PCW biosensor

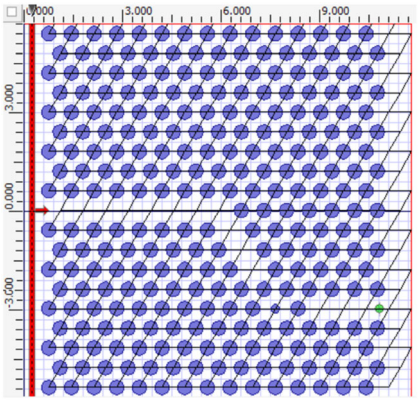

Fig. 9 Design of the Biosensor

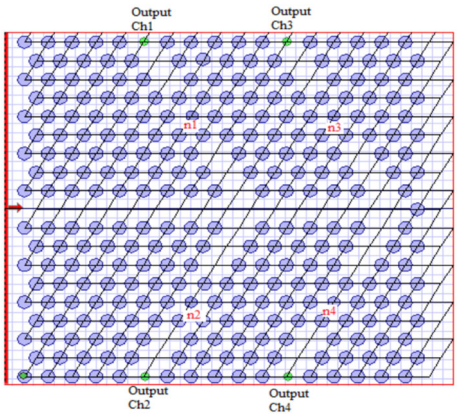

Fig. 10 Biosensor with four different channels

0.5240a/λ to 0.6698a/λ. In this, the defects are introduced by creating a coupled nanocavity within a waveguide. At a guided optical mode a resonant wavelength of 1661 nm is obtained when no analyte is filled within the nanocavity. The optimized structure is by varying the radius of the central nanocavity, shifting the adjacent holes, and by changing the radius of adjacent holes. First, the nanocavity is filled with a healthy person's blood with a refractive index of 1.35 and with different radii of the defect is observed and the optimum radius is taken as 0.16a since it ends up with high sensitivity with good Q factor. Further, optimization is done by shifting the adjacent holes away from the nanocavity and the structure sense the normal and cancer cells with a sensitivity of 388.57 nm and a quality factor of 4856.75. Further there is a wavelength shift in the output spectra according to the change in the refractive index of the cancer cells. Figure 11 represents the 3D view of the biosensor.

Harhouz and Hocini (2015) Proposed a high sensitive biosensor with two waveguides and one microcavity. It is based on the principle of shift in the resonant wavelength due to the change in the refractive index of the liquids such as deionized water (n = 1.33), distilled water (n = 1.3147),

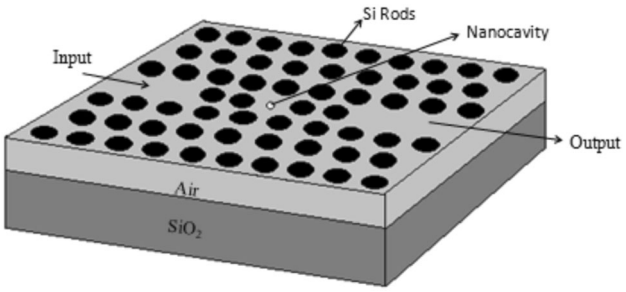

Fig. 11 3D View of dielectric profile of nanocavity coupled waveguide structure

acetone (n = 1.3445), methanol (n = 1.316), isopropyl alcohol (n = 1.363). The structure of the biosensor consists of a triangular lattice with air holes on the dielectric silicon slab with a lattice constant of 470 nm and the radius of the air holes is taken as 190 nm. The Photonic crystal structure shows a bandgap ranges from 1135 to 1860 nm for TM polarization.

To further increase the sensitivity of the sensor the radius (r') of the air holes along the waveguide is optimized to 200 nm as it provides the highest transmittance and quality factor of Q = 1.47 × 10^4. For the change in RI as Δn = 0.001the resonant wavelength changes to 0.435 nm and sensitivity is obtained as S = 425 nm/RIU. Finally, the sensor has a transmission efficiency of 73–84.4%. Figure 12 represents the biosensor.

Hocini and Harhouz (2016) designed a temperature-sensitive biosensor with a triangular lattice of a spatial period of a = 470 nm with airholes on dielectric slab configuration. The radius of the airholes r = 190 nm. The Photonic Band Gap (PBG) is calculated using Plane-wave expansion method (PWE) with a bandgap of 1135 to 1860 nm for TM polarization and for very small TE polarization without defect for 19 × 13 lattice structure. Two waveguide and a microcavity were formed as a defect in the photonic crystal structure. Further to improve the sensitivity the radius (r') of the air holes along each side of the waveguide is varied or simply the width of the waveguide and the cavity by adjusting the no of holes. The

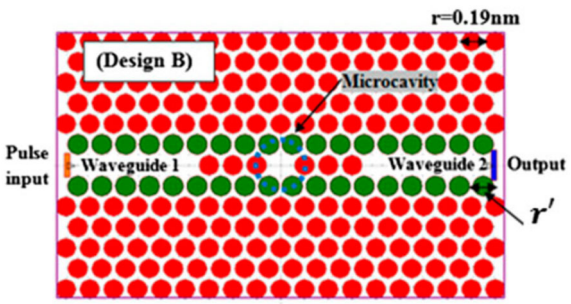

Fig. 12 The biosensor with two waveguide and a microcavity

transmission spectra were calculate using FDTD method for the varying RI from 1.323 to 1.333 corresponding to the change in temperature from T = 90 °C to 20 °C. Thus, the sensor parameters radius (r') along the waveguide and no of airholes were optimized r' = 0.2um and three respectively.

Figure 13 represents the biosensor. As the RI of the distilled water changes for 0.001 with respect to temperature a 0.44 nm shift is visible in resonating wavelength. The temperature sensitivity is defined as $\Delta\lambda/\Delta T$ (pm/°C), a sensitivity of 84 pm/°C for a measurement temperature range between 20 °C and 90 °C.

Sani et al. (2021) have proposed a highly sensitive biosensor for detecting cancer and diabetes using 2D photonic crystals. The host structure composed of Silicon rods in air bed arranged in a hexagonal lattice with a lattice constant a = 600 nm. The radius of the silicon rods is 120 nm. There are two tubes in the structure to place the samples of blood (red tube) and tear (cyan tube) for measurement as shown in Fig. 14 and the radii of the red and cyan tubes are RC1 = 0.9a, and RC2 = 1.1a. From the blood sample, the cancer cells are detected and the tear is used to diagnose diabetes.

Plane-wave expansion method (PWE) is used to obtain the normalized bandgap in TM polarization mode at $0.276 < a/\lambda < 0.446$, which is equal to 1345 nm $< \lambda <$ 2173 nm. The laser source of central wavelength of λ = 1550 nm is applied in the sensor as it is initially filled with the blood and tear of a healthy person with a refractive index of 1.36 and 1.35 placed inside the red and cyan tubes. At resonance, the wavelength is shifted λ_{S1} = 1.562 μm for tear sample and λ_{S2} = 1.593 μm for blood sample. The sensitivity is figured out as S = 3080 nm/RIU and FOM = 1550.11 ± 150.11 RIU^{-1}. The transmission efficiency of 95% and 100% for tear and blood sample respectively.

Three different cancer cells have been analyzed such as Basal cancer cell (epidermis), HeLa cells (HPV18) and MDA-MB-231 (Breast cancer). These cells in normal state

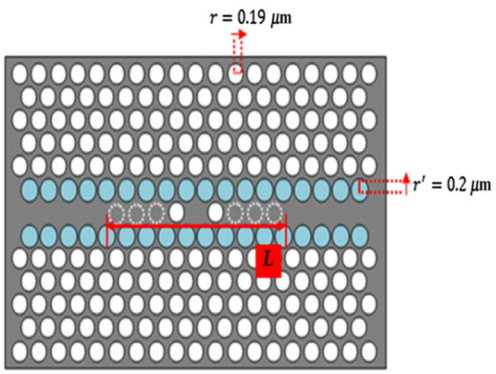

Fig. 13 Biosensor with 2 waveguide, a microcavity, and 3 air holes

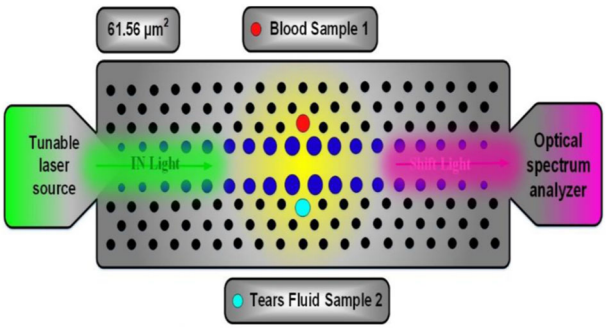

Fig. 14 Biosensor to detect cancer and diabetes

have a refractive index of 1.36, 1.368, and 1.385 and cancerous cells have a refractive index of 1.38, 1.392, and 1.399 respectively. The FOM is 940.475 ± 025 RIU^{-1} with a sensitivity of S = 1893 nm/RIU and Quality factor of 946.5 for Basal cancer cells. For HeLa cancer cells the FOM = 805.283 ± 58.92 RIU^{-1} and sensitivity S = 1642 nm/RIU. The MDA-MB-231is extracted from the human chest from a breast cancer patient. These have a FOM = 1109.51 ± 55.23 RIU^{-1} and S = 2214 nm/RIU. Further, the tear sample is also analyzed and the normal and the diabetic cells have a refractive index of 1.350 and 1.410 respectively with a sensitivity of 1294 nm/RIU.

This structure has a unique feature as two samples can be simultaneously detected using two tubes and the quality factor is obtained as 946.50, FOM as 1109.51 ± 55.235 RIU^{-1} with 100% transmission efficiency and with highest sensitivity of 3080 nm/RIU^{-1}. The detection limit range is 31 × 10^{-6} RIU.

Resonators based biosensors

Resonator-based Biosensors are designed by including cavity, waveguide, and a ring at the center of the resonator. The shape of the ring depends on the application of the senor and the analyte. The rings can be circular, Diamond, elliptical etc. The Resonator based sensors are said to be highly sensitive, lower detection limit and with high-quality factor. Moreover, it requires minimum amount of analyte for the sensing purpose with high transmission efficiency. Further, in some of the resonators, the analytes are filled in a very small sensing area with in the sensor which adds more advantage for these type of sensors.

Kumar et al. (2020) designed a biosensor to detect cervical cancer cells. The sensor has an input and output waveguide with a central ring. Air holes in slab configuration are used with a lattice constant of 450 nm. The holes in the sensor are filled with cervix blood sample cells and change in ERI of the normal and the cancers cells shifts the intensity and the wavelength as 0.0176 and 06 nm

respectively. The quality factor and the sensitivity are observed as 248 and 143 nm/RIU.

Robinson and Dhanlaksmi (2017) proposed a Biosensor with two inverted L waveguide and ring resonator at the center with a foot print of 11.4 μm × 11.4 μm as depicted in Fig. 15. In this, the glucose concentration of the urine is sensed over a range of 0-15gm/dl. The basic principle behind the sensing is the change in refractive index of the urine as the glucose concentration in the urine is varied and the corresponding output response of the sensor is varied. The structure consists of 21 × 21 square lattice with a lattice constant of 540 nm. Silicon rods in air configuration are used with the radius of the rods is 100 nm. The TM polarization Photonic Band Gap (PBG) exists over a range of 0.435 a/λ to 0.295 a/λ and its respective wavelength is given as 1241 nm to 1830 nm for the Photonic crystal structure without defects. When defects such as two inverted L-shaped waveguides and one ring resonator are introduced the PBG is broken and the Guided modes propagate into the region. The circular ring resonator has an inner radius of 50 nm and outer radii of 100 nm. However, the Si rod placed in the top and bottom of the ring resonator is 86 nm in order to improve the output transmission. At resonance the signal from the input L waveguide is coupled to the ring resonator and reaches the output L waveguide. The resonating wavelength is 1545 nm, transmission efficiency is 100% and quality factor is obtained as 256 at normal condition.

The output spectra of the designed sensor for different glucose concentration in urine ranges from 0.625 to 5 gm/dl, and it can be noted that the output power decreases as the urine glucose concentration increases. For normal level (0–15 mg/dl) the quality factor is obtained as 264 at a resonating wavelength of 1585 nm with 100% transmission efficiency. As the glucose concentration increases to 5gm/dl the transmission spectra is only 55% and the quality factor is 217 at the same resonating frequency. It is also observed that the refractive index of the blood also increases as the glucose concentration in blood increases. For normal glucose level (165–180 mg/dl) The quality factor is obtained as 264 with 100% transmission efficiency at a wavelength of 1585 nm. As the glucose level increases to 342 mg/dl the output transmission power reduce to 75% and the quality factor is achieved as 269 at the same resonating wavelength.

Robinson and Nakkeeran (2012b) designed a salinity sensor using 2D photonic crystal ring resonator (PCRR) for monitoring the salinity of the seawater from 0 g/L to 100 g/L at 25 °C. The sensor consists of Si rods in air bed with a square lattice, the radius of the rods is 0.185xa where a is the lattice constant and selected as 540 nm. The central circular ring resonator is coupled with two inline quasi waveguides and single coupling rod is placed at either side of the quasi waveguide. One coupling rod at the input and output side was optimized as it provides the high output power of 99.5%, with a high Q-factor of 478 at a wavelength of 1590.5 nm at 0% salinity. Now as the salinity increases for every 5% in seawater the output power spectra reduce to 2.69% approximately, as different salinity has different refractive index which leads to change in the output power of the sensor at 25 °C. The minimum detectable range of the sensor is 1% (1 g/L) and 100% for a temperature of 5 °C and 25 °C. The below Fig. 16 depicts the PCRR sensor and the normalized output spectrum is obtained at different salinity at 25 °C.

Chhipa et al. (2017) designed the 2D PC based Micro Cavity Ring Resonator Sensor to detect the glucose concentration The sensor is designed with Hexagonal lattice and air holes in dielectric slab. The sensor consists of Ring Resonator, the resonator designed to drop the unique wavelength with change in the refractive index of the glucose concentration in urine. The design had 100% Transmission Efficiency for 1551 nm with Q factor of 272. The Resonator shifts the resonant wavelength based on the

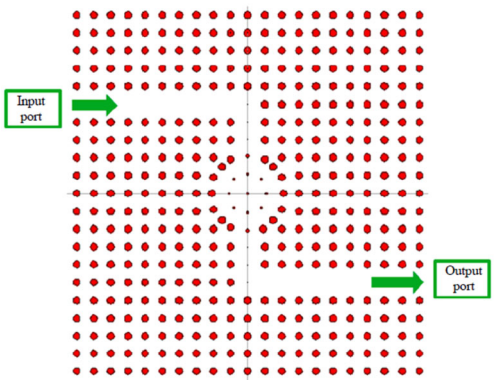

Fig. 15 Biosensor with two inverted L waveguide and one ring resonator

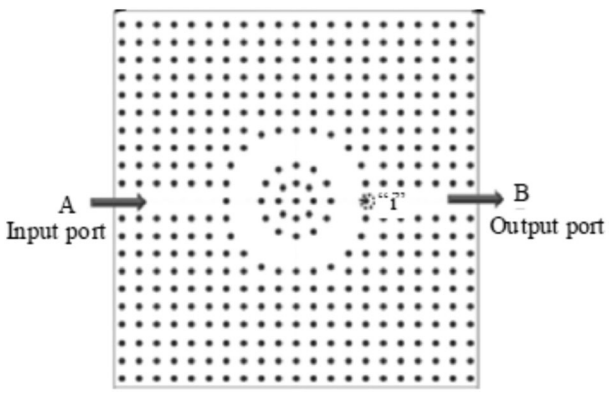

Fig. 16 PCRR sensor

changes in refractive index of the glucose concentration in the urine. Figure 17 represents the biosensor.

Arunkumar et al. (2019) proposed a 2D PC-based Biosensor to Detect Different Blood Components such as Red Blood cells, White Blood Cells, Hemoglobin, Blood sugar, etc. The wavelength of the Blood constituents ranges from 1530 to 1615 nm. A Photonic crystal Ring Resonator based sensor is designed with cubic lattice and Rods in air configuration is used with a lattice constant of 540 nm and it has a unique elliptical-shaped resonator at the center of structure and the circular rod front and back radius is 100 nm. Plane-wave expansion method (PWE) is used for calculating the Photonic Band Gap (PBG) and FDTD method is used to obtain the transmission spectra and field distribution. At normal condition when light is propagated in elliptical-shaped resonator through the waveguide and the normalized transmission spectrum is measured at the output and the resonating wavelength, Q-factor, and the transmission efficiency is measured as 1590 nm, 257.5, and 100% respectively. The output transmission spectra, resonating wavelength changes with respect to the change in the refractive index of different blood constituents when the analytes are placed on the sensor. Thus, the Q-factor, Transmission efficiency and Detection limit with elliptical-shaped resonator PCRR are reported as 262, 97%, and 0.002RIU^{-1} for different blood components. Figure 18 depicts the elliptical biosensor.

Arafa et al. (2017) proposed a 2D PC with triangular lattice of air holes etched in silicon slab with a radius of 0.37a where a is the lattice constant of the Photonic crystal structure (a = 530 nm). The thickness of the silicon slab is taken as h = 230 nm. The low index SiO_2 (n = 1.45) lying beneath the high index Si slab (n = 3.45) has a thickness of 1500 nm helps the confinement of light within the cavity core, preventing optical losses into the lower substrate and ensure the total internal reflection in the vertical direction. The photonic bandgap (PBG) ranges from 0.278(a/λ) and 0.4(a/λ) for TE polarization and it corresponds to a

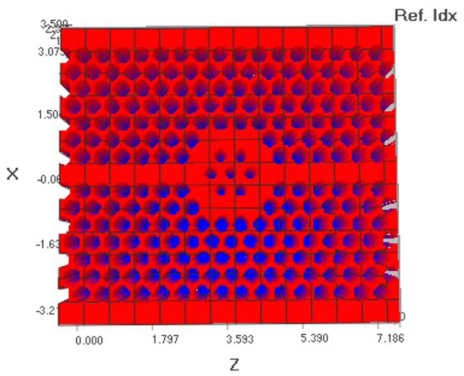

Fig. 17 Schematic structure of proposed photonic crystal-based biosensor

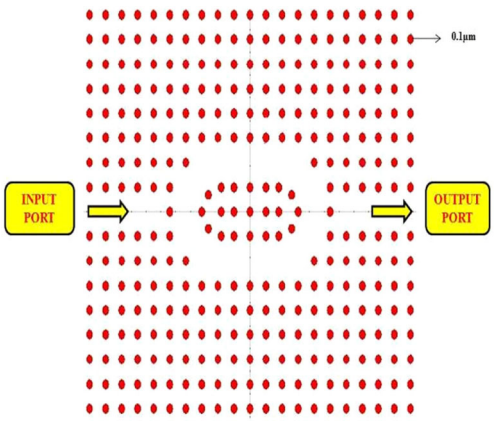

Fig. 18 Proposed biosensor using elliptical ring resonator

wavelength range of 1323.7–1908.1 nm. The device consists of two waveguide couples and one cavity which has ring-shaped holes etched in the Si layer. This ring-shaped holes have the inner and outer radius as R_{in} = 126.5 nm (0.23a) and R_{out} = 247.5 nm (0.45a) respectively, thus the ringed air region is given by Rout − Rin = 121 nm. Figure 19a shows the PC biosensor on SOI substrate and 19b shows the ring-shaped cavity with input and output waveguide.

The spectral response of the cavity without the sample is obtained and λ = 1373.7 nm is chosen for high Q factor of 7.06×10^3. Initially, the sensing is done by local infiltration of de-ionized (DI) water in the cavity sensing region which corresponds to the change in the refractive index of the ring-shaped holes from 1(air) to 1.33 (DI water). This change corresponds to the spectral red-shift of 140.7 nm and the RI sensitivity as 426.36 nm/RIU.

For obtaining high Q-factor and sensitivity S, the sensor is designed at R_{in} = 0.255a. The magnitude of the resonant wavelength shift depends upon the number of functionalized holes and change in the refractive index of the targets. For optimal Q -factor and sensitivity S the functional holes is taken as N = 4, in which the analytes are filled with glucose solution is indicated as blue circular holes as shown in Fig. 20

The glucose solution concentration is varied from (0, 10, 20, 30, 40, 50, 60) g/L and its corresponding refractive index is varied and the corresponding wavelength shift is obtained. The sensor generates a very good result at λ = 1571.0 nm the sensitivity is obtained as 462.61 nm/RIU, high Q-factor as 1.112×10^5, resulting in a detection limit less than 3.03×10^{-6} RIU. Plane wave expansion is used for calculation of the photonic band gap and 2D-FDTD is used for the structural analysis of the sensor.

Areed et al. (2017) proposed a highly sensitive photonic crystal refractometer for monitoring the glucose concentration with a face-shaped biosensor in which the defect is

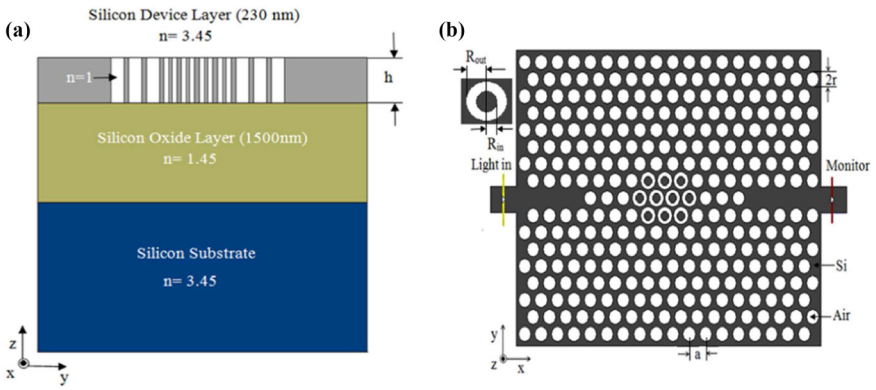

Fig. 19 **a** Schematic side sectional view of the PhC biosensor structure in SOI substrate. **b** Schematic diagram of the ring-shaped photonic crystal cavity coupled to an input and output PhC waveguides

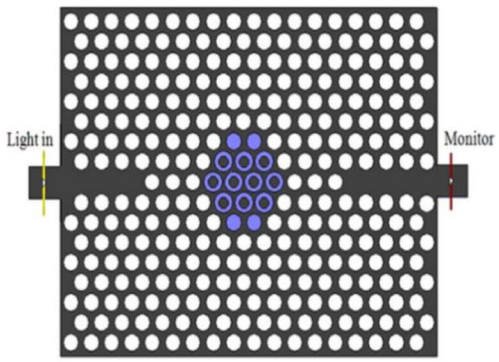

Fig. 20 The optimal PhC biosensor structure, the blue shapes refer to the sensing area filled with glucose solution

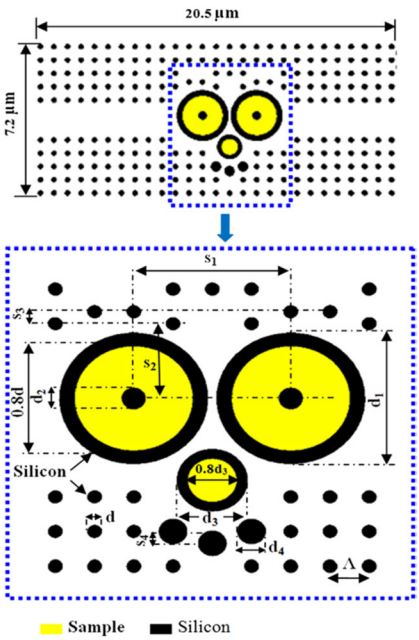

Fig. 21 face-shaped PhC biosensor

filled with analyzed analyte. The photonic crystal is designed on a silicon on insulator (SOI) platform which has 1 µm thick silicon slab (n = 3.4) on the top of silicon dioxide layer (n = 1.45) placed on a silicon substrate. The biosensor consists of silicon rods with a height of 1 µm arranged in a square lattice with a lattice constant of 0.58 µm and a central waveguide is formed by removing two row of silicon rods in the center. In addition, two large hollow cylinders filled with the analytes are used with inner and outer diameters of $0.8d_1$ and d_1, respectively. Further, the two hollow cylinders have central silicon rod of diameter d_2 and the horizontal distance between the centers of the two cylinders is taken as S_1. Moreover, third hollow cylinder of inner and outer diameters of $0.8d_3$ and d_3 respectively is also filled with the analyte. The Fig. 21 represents the face-shaped biosensor. The parameters of the sensor is optimized as d as 208 nm, d_1 as 6d, d_2 as 2d, d_3 as 5d, d_4 as 2d, S_1 as 2720 nm, S_2 as 860 nm, S_3 as 200 nm, S_4 as 200 nm, and the thickness of the SiO_2 as 300 nm. 3D-FDTD with Perfectly matched layer as boundary condition is used to calculate the photonic bandgap (PBG) for the Photonic crystal structure for TM polarization mode. The PBG ranges from 1.45–1.55 µm. In order to increase the sensitivity of the sensor the analytes are filled in the selected holes forming a micro-fluidic system with incorporating micro-holes. Therefore, as the refractive index of the infiltrated holes varies and hence the spectral transmission through the suggested structure is also changed.

The transmission spectra are obtain and the power spectra of the sample are taken with a refractive index of n = 1.33 with Si rods of height 1 µm and it is observed that not less than 15% of the incident power is lost in the vertical direction which indicates the effectiveness of the biosensor.

As the face-shaped cavities are filled with the analyte sample of glucose solution with different refractive index, n = 0.00011889C + 1.33230545 where C is the glucose concentration (g/L). Now as the glucose concentration is varied from 30 to 300 g/L there is linear shift in the resonant wavelength as the analyte refractive index varies from 1.3359 to 1.3715 and good sensitivity is obtained as

359 nm/RIU. The quality factor and the detection limit are achieved as 477 and 10^{-6} RIU respectively.

Huang et al. (2014) proposed a novel biochemical sensor structure of photonic crystal Ring defect coupled resonator (RDCR). The structure employs a triangular lattice, air holes arranged in silicon slab of refractive index of 3.48. The ring resonator cavity and quasi waveguide were formed by removing few holes on the Si slab. Figure 22 represents the sensor with a lattice constant of 348 nm, hole radius r as 0.34a, and thickness of the slab as 0.55a. A TE-like polarized light is coupled in the input quasi waveguide and unique resonating wavelength is chosen at 1552.34 nm (0.2646 (2πc/a)) as the structure refractive index changes there is a shift in the resonating wavelength. The highest quality factor was achieved by adjusting the width of the line defect of the waveguide and by altering the radius of the air hole inside the ring resonator. In Fig. 23 red hole depicts the radius of the air hole in the ring resonator and was optimized to 0.40a as it gives the highest quality factor of 6.93×10^6 at normalized frequency of 0.2672 (2πc/a). The blue air holes indicate line defect width W of the sensor and it is modulated by varying the width to W = 0.985W1 as the high Q factor is obtained as 1.86×10^7. The whole simulation was employed in 3D-FDTD. The various refractive index is used for calculation purpose such as n = 1.315, n = 1.330 (deuterium water) and n = 1.345 (glycerol solutions).

To improve the sensitivity of the sensor the no of inner ring holes is altered as $N_{in} = 7$ and the total functional holes along with the inner holes are optimized as N = 25. The analytes are filled in the yellow shaded are alone as shown in Fig. 24 and in the output spectra there are a linear shift in the wavelength as the refractive index of the sensor varies.

In addition, the effect of fabrication roughness is also considered and the simulation is done underwater environment. The Quality factor is obtained as Q = 35,517 for a random roughness of air holes is about 20 nm. The sensitivity is achieved as 300 nm/RIU and a high figure of merit of ~ 8000. The Detection Limit is achieved as 1.24×10^{-5}.

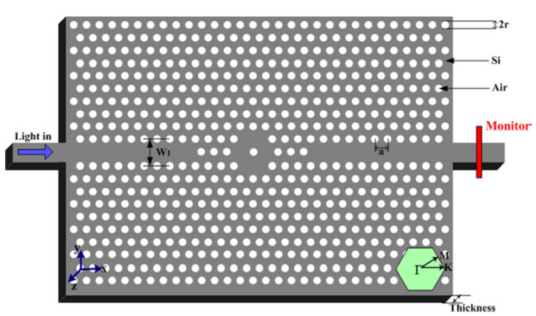

Fig. 22 Proposed biosensor

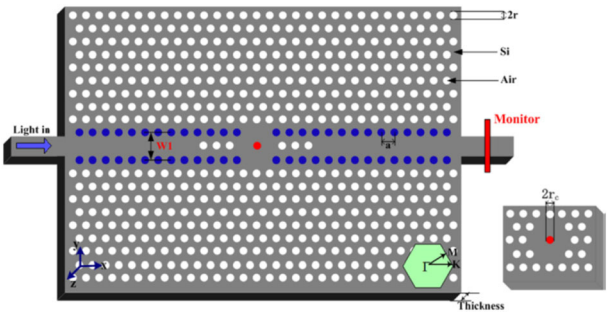

Fig. 23 The red hole radius $r_c = 0.40a$ and the blue air holes width W = 0.985W1

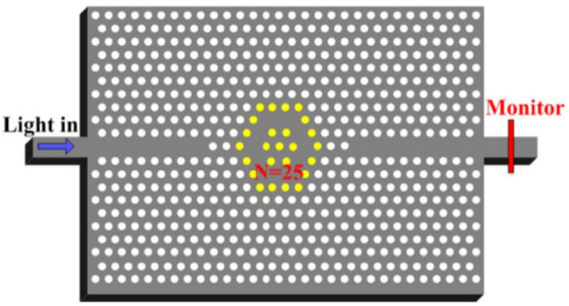

Fig. 24 Ring defect coupled resonator structure with N = 25 functional holes

Chopra et al. (2016) designed a diamond-shaped ring resonator with bus and drop waveguide. This sensor is used to detect different diseases with respect to the analyte such as blood, urine, tears, etc. It has a hexagonal lattice with Si rods in air configuration, with the radius of the rods as 120 nm and a lattice constant of 410 nm. The rod size in the line defect i.e., in bus and drop waveguide and along the diamond-shaped ring resonator is reduced to 30 nm as shown in Fig. 25. The input wavelength is taken as 1550 nm as the PBG is obtained for the defect-free lattice as 1278 nm to 1619 nm. In the diamond-shaped resonator, there is central cylinder with the inner and the outer radius as 180 nm and 200 nm respectively. The inner hole of the ring-shaped middle cylinder is filled with the analyte and as the light is applied in the bus waveguide and the change in refractive index is monitored at the drop waveguide which corresponds to the shift in the resonate wavelength. Various analyte such as Basal cell, HeLa cell, MDA-MB-231 cell both for normal and cancer cells, tears and blood components are bonded in the sensing region and the transmission spectra are recorded. The average quality factor is identified as 1082.2063.

Swain and Palai (2016) proposed a honeycomb structure in 2D photonic crystal to estimate the hemoglobin concentration in the human blood via Arduino development board consist of Atmega 320 microcontroller. Figure 26 represents the honeycomb structure of the PC with a

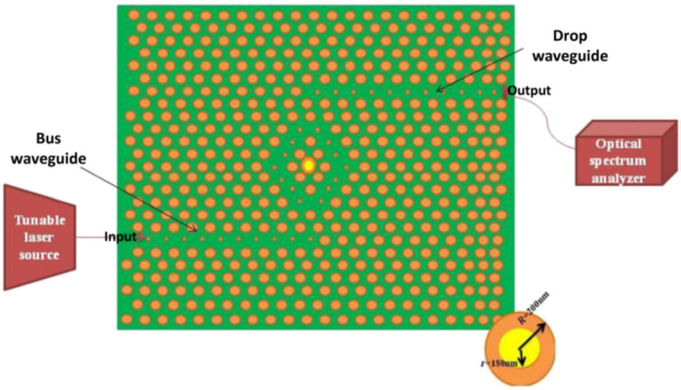

Fig. 25 The diamond resonator with bus and drop waveguide

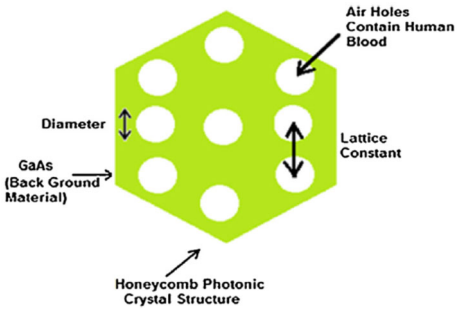

Fig. 26 Honeycomb PC structure

background material as Gallium Arsenide containing air holes. There are about 9 air holes in the proposed structure with diameter of 420 nm and lattice spacing of 1um. When the light is incident on the PC of wavelength 589 nm and the honeycomb structure is filled with different percentage of hemoglobin then some amount of energy is reflected and some amount of energy is absorbed and remaining is transmitted through the structure. The linear variation of absorbance and reflected energy is basic principle behind the measurement of the concentration of hemoglobin in blood. Thus, the transmitted energy also varies linearly with respect to hemoglobin concentration. Now the reflected energy is calculated using Plane wave expansion method. An experimental set up was proposed as shown in Fig. 27 to determine the concentration of hemoglobin in both oxygenated and deoxygenated blood ranges from 0 g/L to 120 g/L based on the potential of the transmitted energy of the light which is collected at the Arduino board. This potential varies for different concentration of the hemoglobin. Thus, a graph is drawn between concentration of hemoglobin and transmitted energy in eV and the graph decreases linearly from 0 g/L to 120 g/L with respect to the transmitted signal. For oxygenated blood the transmitted energy decreases from 0.460μeV to 0.4596μeV and for deoxygenated blood 0.460μeV to 0.4434μeV.

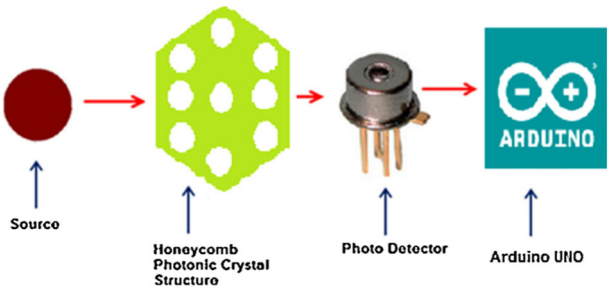

Fig. 27 Experimental setup to measure concentration of Hemoglobin

Suganya and Robinson (2017) has proposed a Rhombic ring resonator to measure the concentration of glucose. The rhombic resonator is designed with biperiodicity (reducing the radii of certain group of rods). It consists of hexagonal lattice of circular rods in air configuration with a bus and dropping waveguide. Along the waveguide, the radii of the rods are about 50 nm and the center of the resonator has two rings such as inner and the outer ring both are of 105 nm respectively. The central elliptical rod is about 150 nm. The lattice constant a = 547 nm with Si rods radius 0.1 μm are used.Fig. 28 represents the rhombic ring resonator. Before introducing the point and line defect the PBG is obtained for TE mode with a wavelength range from 1125 to 1725 nm. As the light is applied at the input port and the sensor is filled with the glucose sample the

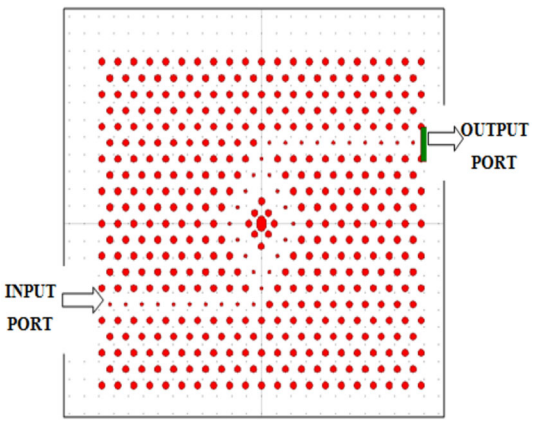

Fig. 28 Rhombic ring resonator

light-matter interaction occurs and there is a change in the resonant wavelength to the corresponding change in the refractive index of the glucose level. At 0 g/L the resonant wavelength, quality factor and transmission efficiency is obtained as 1545 nm, 171.6, and 100% respectively. As the glucose concentration is increased for every 30 g/L from 0 g/L to 330 g/L there is shift of about 2.5 nm in the resonating wavelength. The maximum sensitivity, quality factor, and transmission efficiency are achieved as 1000 nm/RIU, 178, and 100% respectively. The resonator operates in wavelength range of 1540 to 1560 nm.

Olyaee and Mohebzadeh-Bahabady (2014) Proposed a two-curve-shaped nano-ring resonator placed in-between two waveguides. A hexagonal lattice of air holes on dielectric slab configuration is used. The lattice constant is considered as 410 nm and the air hole radius is equal to 120 nm. Two-line defects are introduced to form two waveguides (input and output waveguide) and about 6 sensing holes are used around the central holes of the two ring resonators as depicted in Fig. 29. As the analyte bind in the sensing holes, the intensity of the transmission spectra decreases and this property is used to find the analyte. The PBG for hexagonal lattice is obtained for TM polarization from 1205 nm 1640 nm. To obtain the best sensing hole from SH_1 to SH_6 the holes are varied from 1 to 1.33 (water) and then it is varied from 1 to 1.45 (DNA molecule). The corresponding quality factor, intensity of transmission spectra, and sensitivity are tabulated. The sensing hole SH_1 has a higher sensitivity as 4.125/RIU but SH_5 has a high-quality factor of 1740 and sensitivity of 3.471/RIU with lower intensity shift.

Detail comparison study given in Table 1. From the literature study, it is inferred that each and every work reported with different sensing principle, the sensing principle are broadly categorized into square, triangular lattice, sensor output based on resonance wavelength shift and intensity modulation, and operating mechanism classified into resonator shape-based, line and point defects, constructive and destructive interference based.

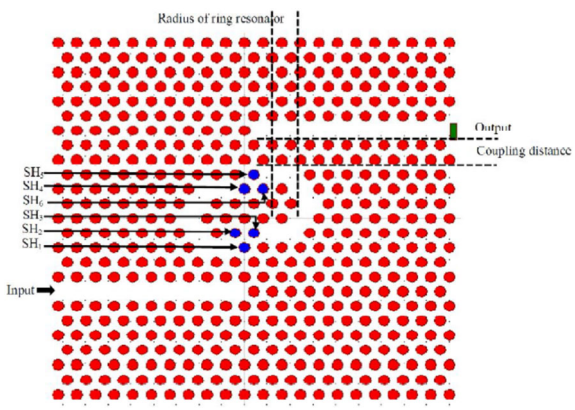

Fig. 29 Two-curve-shaped ring resonator biosensor

For good performance, the sensors should produce efficient performance parameters like sensitivity, quality factor, detection limit, FOM, transmission efficiency, and size of the device. Many proposed designs satisfy the best performance by changing the design structure and the material. But still, shortfalls are not addressed for more analyte. The performance parameter requirements change based on the application. Hence in the future PC sensors can be designed and proposed to satisfy the application based on the standard performance parameters also considering the fabrication limitations.

Future design considerations

Based on above review of the PC based biosensors, it can be inferred that:

Both square and hexagonal lattice structures are used for designing biosensors. Among these, the hexagonal lattice is used in most of the sensors as they provide a wider photonic bandgap. The shape of the rods and holes are mostly preferred as a Circular one as they decrease the fabrication complexity. Rods in air and holes in air slab are used in designing the sensor but the rods in air configuration are widely used. GaAs/ Si/ Si_3N_4 are the materials used in designing the sensor (Painam et al. 2016). But almost all the sensors are designed with Silicon as the predominant material which results in low losses. The performance parameters of the sensors are greatly enhanced by varying the radius of the rod(s) / hole(s) of the nanocavity or by adjusting the width of the line defect or by adjusting the radius of the inner holes or rods of the ring resonator in order to shift the resonating wavelength. Further certain designs are very peculiar in which the analytes are filled at a specific region of sensors and the analysis is done based on the requirement of the designer. Moreover, in some biosensors, two different analytes are placed on the same sensor at different positions and the analysis is done at the same time which is said to be time-consuming and efficient too.

Conclusions

Over the past two decades, photonic crystal-based biosensors are showing a vital role to be played in the field of medical diagnosis, life science, and other applications owing to their high sensitivity, compactness, and high Q-factor. Researchers have designed variety of PC based

Table 1 Comparison of type of lattice, footprint, configuration, rod/hole shape, lattice constant, rod/hole radius, material, RI, structure type, Sensitivity, Quality factor, detection limit, Figure of Merit, Transmission efficiency, and Sensing Principle of the Photonic Crystal sensor with the reported one

Ref.no	References	Footprint	Lattice structure	Configuration	Rod shape/Holes shape	Lattice constant (a) (nm)	Radius of rods®/holes (nm)	Material used for	RI of Si
23	Krupa and Triveni (2020)	6 × 6 μm^2	Square	Rods in air	Circular	540	100	Si	3.46
31	Nischita et al. (2015)	–	Square	Rods in air	–	0.99	0.2	Si	k of Si is 12
49	Sharma and Sharan (2014a)	–	Hexagonal	Rods in air	Circular	100	170	Si	k of Si is 12
50	Sharma and Sharan (2015)	–	Hexagonal	Holes in slab	–	100	420	Si	k of Si is 12
50	Sharma and Sharan (2015)	15 × 20 matrix	Square	Rods in air	Circular	100	190	Si	–
53	Sundhar et al. (2019)	21 × 21 Matrix	Square	Rods in air	Circular	588	80 (size of the rod)/ 40	Si	3.45/rod
24	Kulkarni et al. (2020)	–	Square	Rods in air	Circular	1000	–	Si	k = 12
47	Sharma and Sharan (2014b)	–	Square	Rods in air		1000	190	Si	–
34	Painam et al. (2014)	–	Hexagonal	Holes in slab	Circular	1000	200	Si	3.49
35	Painam et al. (2016)	–	Hexagonal	Holes in slab	Circular	1000	450	GaAs/Si/ Si3N4	
1	Ameta et al. (2017a)	19 × 15μm^2	Hexagonal	Rods in air	Circular	690	220	Si	3.673
2	Ameta et al. (2017b)	19 × 17μm^2	Hexagonal	Rods in air	Circular	680	200	Si	3.673
18	Jindal et al. (2016)	19 × 12 μm^2	Hexagonal	Rods in air	Circular	800	240	Si	3.42
15, 16	Hocini and Harhouz (2015, 2016)	–	Hexagonal	Holes in slab	Circular	470	190	Si	3.45
16	Hocini and Harhouz (2016)	–	Hexagonal	Holes in slab	Circular	470	190	Si	3.45
46	Sani et al. (2021)	61.56 μm^2	Hexagonal	Rods in air	Circular	600	120	Si	3.45
25	Kumar et al. (2020)	8 × 6 μm^2	Hexagonal	Holes in slab	Circular	450	120	Si	3.45
42	Robinson and Dhanlaksmi (2017)	11.4 × 11.4 μm^2	Square	Rods in air	Circular	540	100	Si	3.46
44	Robinson and Nakkeeran (2012b)	–	Square	Rods in air	Circular	540	100	Si	3.46
11	Chhipa et al. (2017)	6.42 × 7.27 μm^2	Hexagonal	Holes in slab	Circular	428	149.8	Si	3.47
5	Arunkumar et al. (2019)	11.4 × 9.2 μm^2	Square	Rods in air	Circular	540	100	Si	3.46
3	Arafa et al. (2017)	–	Hexagonal	Holes in slab	Circular	530	196	Si	3.45
4	Areed et al. (2017)	7.2 × 20.5 μm^2	Square	Rods in air	Circular	580	104	Si	3.45
17	Huang et al. (2014)	–	Hexagonal	Holes in slab	circular	348	118	Si	3.48
12	Chopra et al. (2016)	–	Hexagonal	Rods in air	Circular	410	120	Si	–
55	Swain and Palai (2016)	–	Hexagonal-Honeycomb	Holes in slab	Circular	1000	210	GaAs	–

Table 1 (continued)

Ref.no	References	Footprint	Lattice structure	Configuration	Rod shape/Holes shape	Lattice constant (a) (nm)	Radius of rods®/holes (nm)	Material used for	RI of Si
52	Suganya and Robinson (2017)	11.4 × 9.8 μm^2	Hexagonal	Rods in air	Circular	547	100	Si	3.45
32	Olyaee and Mohebzadeh-Bahabady (2014)	–	Hexagonal	Holes in slab	Circular	410	120	Si	2.825

Ref.no	References	Structure type	Sensitivity	Quality factor	Detection limit	FOM	Trasmission efficiency	Senses
23	Krupa and Triveni (2020)	Waveguide	–	–	–	–	–	Change in RI of urine of pregnant women by the detection of Human Chorionic gonodotrophin(HGC)
31	Nischita et al. (2015)	Waveguide	1×10^{-6}	118,563	–	–	–	Breast Cancer cell DNA
49	Sharma and Sharan (2014a)	Waveguide	–	–	–	–	–	Concentration of Glucose in urine is detected
50	Sharma and Sharan (2015)	Waveguide	638 nm /RIU	23,575	–	–	–	Glycosuria in urine and Diabetes mellitus in blood are detected
50	Sharma and Sharan (2015)	Waveguide	–	–	–	–	–	Basal, Breast and Cervical cancer cells
53	Sundhar et al. (2019)	L and inverted L wavwguide	523.81	110.53	–	–	100%	Senses cervical cancer cells
24	Kulkarni et al. (2020)	Waveguide	–	–	–	–	–	Senses the bacteria in contaminated water with the change in RI
47	Sharma and Sharan (2014b)	Line defect	–	–	–	–	–	Lymphocyte Cell
34	Painam et al. (2014)	Waveguide	–	–	–	–	–	Concentration of sulphuric acid
35	Painam et al. (2016)	Waveguide	2.02 nm/RIU	–	–	–	–	Detects E.coli
1	Ameta et al. (2017a)	Waveguide and nanocavity	–	–	–	–	–	A nano-cavity coupled waveguide biosensor is proposed to detect different blood components such as cytop, Blood plasma etc

Table 1 (continued)

Ref.no	References	Structure type	Sensitivity	Quality factor	Detection limit	FOM	Trasmission efficiency	Senses
2	Ameta et al. (2017b)	Drop waveguide and nanocavity	–	–	–	–	–	Senses the Glucose level in Blood with four drop waveguide and sensing holes
18	Jindal et al. (2016)	Waveguide and nanocavity	388.75 nm/RIU	4856.75	–	–	–	Sensos five different cancer cells with high sensitivity and reasonable Q factor
15, 16	Hocini and Harhouz (2015, 2016)	Waveguide and microcavity	425 nm/RIU	1.47×10^4	–	–	73–84.4%	Different liquids
16	Hocini and Harhouz (2016)	waveguide and microcavity	84 pm/°C	–	0.001 RIU^{-1}	–	–	Temperature sensor
46	Sani et al. (2021)	Waveguide and microcavity	1294–3080 nm/ RIU^{-1}	946.5	31×10^{-6} RIU	1109.51 ± 55.235 RIU^{-1}	100%	Blood and tears for detection of cancer and diabetes
25	Kumar et al. (2020)	Waveguide with central ring	143 nm/RIU	248	–	–	–	Cervix cancer cell
42	Robinson and Dhanlaksmi (2017)	L waveguide and ringresonator	–	257	–	–	100%	Glucose, albumin, urea and bilirubin concentration in urine and glucose concentrayion in blood
44	Robinson and Nakkeeran (2012b)	Waveguide and ring resonator	1%(1 g/L) and 100% for a temperature of 5 °C and 25 °C	478	–	–	99.50%	Salinity of seawater at different temperature
11	Chhipa et al. (2017)	Microcavity ring resonator	–	272	–	–	–	A 2D Pc based micro cavity Ring Resonator sensor to detect the glucose concentration in urine
5	Arunkumar et al. (2019)	Elliptical ring resonator	262	–	0.002 RIU–1	–	97%	Blood components
3	Arafa et al. (2017)	Ring shaped cavity with waveguides	462.61 nm/RIU	1.112×10^5	DL = 3.03×10^{-6} RIU	–	–	Glucose concentration
4	Areed et al. (2017)	Face shaped biosensors	359 nm/RIU	477	DL = 10^{-6} RIU	–	–	Glucose concentration
17	Huang et al. (2014)	Hexagonal ring resonator	300 nm/RIU	35,517	1.24×10^{-5}	8000	–	Deuterium water and glycerol solutions

Table 1 (continued)

Ref.no	References	Structure type	Sensitivity	Quality factor	Detection limit	FOM	Trasmission efficiency	Senses
12	Chopra et al. (2016)	Diamond shaped resonator	–	Average QF = 1082.2063	–	–	–	cancer cells, tears and blood components
55	Swain and Palai (2016)	Honeycomb photonic crystal structure	–	–	–	–	–	Measure concentration of Hemoglobin
52	Suganya and Robinson (2017)	Rhombic ring resonator	1000 nm/RIU	178	–	–	100%	Measure the concentration of glucose
32	Olyaee and Mohebzadeh-Bahabady (2014)	Two curved shaped ring resonator	3.741 /4.125	1740/1550	–	–	–	DNA molecule

k = dielectric constant

biosensors with point, line defects, and ring resonators to meet the requirement of the problem identified and to achieve high-quality factor, figure of merit, sensitivity, detection limit, and transmission efficiency. Out of these various designs only very few meet the required performance parameters. However, there is a lot of scope for modifying, improving the designs meeting fabrication limits and packaging of PC-based biosensors for biomedical applications. In future novel designs such as multiple diseases detecting biosensors on a single sensor chip with minimum complexity and better performance will be the potential research area in PC-based sensors.

References

Ameta S, Sharma A, Inaniya PK (2017a) Nanocavity coupled waveguide photonic crystal biosensor for detection of different blood components. In: 2017 international conference on computing, communication and automation (ICCCA) (pp 1554–1557). IEEE

Ameta S, Sharma A, Inaniya PK (2017b) Designing a multichannel nanocavity coupled photonic crystal biosensor for detection of glucose concentration in blood. In: 2017 8th international conference on computing, communication and networking technologies (ICCCNT) (pp 1–4). IEEE

Arafa S, Bouchemat M, Bouchemat T, Benmerkhi A, Hocini A (2017) Infiltrated photonic crystal cavity as a highly sensitive platform for glucose concentration detection. Opt Commun 384:93–100

Areed NF, Hameed MFO, Obayya SSA (2017) Highly sensitive face-shaped label-free photonic crystal refractometer for glucose concentration monitoring. Opt Quant Electron 49(1):1–12. https://doi.org/10.1007/s11082-016-0847-9

Arunkumar R, Suaganya T, Robinson S (2019) Design and analysis of 2D photonic crystal based biosensor to detect different blood components. Photon Sensors 9(1):69–77

Bahaddur I, Tejaswini MR, Santhosh Kumar TC, Sharan P, Srikanth PC (2019) 2D Photonic crystal cantilever resonator pressure sensor. In: 2019 workshop on recent advances in photonics (WRAP) (pp 1–4). IEEE

Balaji VR, Murugan M, Robinson S (2016) Two-dimensional photonic crystal assisted DWDM demultiplexer with uniform channel spacing. Dig J Nanomater Biostruct 11(4)

Bayindir M, Temelkuran B, Ozbay EJAPL (2000) Photonic-crystal-based beam splitters. Appl Phys Lett 77(24):3902–3904

Bougriou F, Boumaza T, Bouchemat M (2014) Design of photonic crystals waveguide using microfluidic infiltration. In: Applied mechanics and materials (vol 492, pp 301–305). Trans Tech Publications Ltd

Chao CY, Fung W, Guo LJ (2006) Polymer microring resonators for biochemical sensing applications. IEEE J Sel Top Quantum Electron 12(1):134–142

Chhipa MK, Robinson S, Radhouene M, Najjar M, Srimannarayana K (2017) 2D photonic crystal micro cavity ring resonator based sensor for biomedical applications. In: 2017 conference on lasers and electro-optics pacific rim (CLEO-PR) (pp 1–2). IEEE

Chopra H, Kaler RS, Painam B (2016) Photonic crystal waveguide-based biosensor for detection of diseases. J Nanophoton 10(3):036011

Chow E, Grot A, Mirkarimi LW, Sigalas M, Girolami GJOL (2004) Ultracompact biochemical sensor built with two-dimensional photonic crystal microcavity. Opt Lett 29(10):1093–1095

Clark LC Jr, Lyons C (1962) Electrode systems for continuous monitoring in cardiovascular surgery. Ann N Y Acad Sci 102(1):29–45

Harhouz A, Hocini A (2015) Design of high-sensitive biosensor based on cavity-waveguides coupling in 2D photonic crystal. J Electromagnet Waves Appl 29(5):659–667

Hocini A, Harhouz A (2016) Modeling and analysis of the temperature sensitivity in two-dimensional photonic crystal microcavity. J Nanophotonics 10(1):016007. https://doi.org/10.1117/1.JNP.10.016007

Huang L, Tian H, Yang D, Zhou J, Liu Q, Zhang P, Ji Y (2014) Optimization of figure of merit in label-free biochemical sensors by designing a ring defect coupled resonator. Opt Commun 332:42–49. https://doi.org/10.1016/j.optcom.2014.06.033i

Jindal S, Sobti S, Kumar M, Sharma S, Pal MK (2016) Nanocavity-coupled photonic crystal waveguide as highly sensitive platform for cancer detection. IEEE Sens J 16(10):3705–3710

Joannopoulos JD, Villeneuve PR, Fan S (1997) Photonic crystals: putting a new twist on light. Nature 386(6621):143–149

Joannopoulos JD, Johnson SG, Winn JN, Meade RD (2008) Molding the flow of light. Princeton University Press, Princeton

John S (1987) Strong localization of photons in certain disordered dielectric superlattices. Phys Rev Lett 58(23):2486

Kok AA, van der Tol JJ, Baets R, Smit MK (2009) Reduction of propagation loss in pillar-based photonic crystal waveguides. J Lightwave Technol 27(17):3904–3911

Krupa V, Triveni CL (2020) Design of biosensor for the detection of pregnancy based on hcg presence in urine using photonic crystal waveguide. In: 2020 IEEE international conference on electronics, computing and communication technologies (CONECCT) (pp 1–4). IEEE

Kulkarni S, Khan N, Sharan P, Ranjith B (2020) Bacterial analysis of drinking water using photonic crystal based optical sensor. In: 2020 7th international conference on computing for sustainable global development (INDIACom) (pp 186–191). IEEE

Kumar H, Vaibav AM, Srikanth PC (2020) 2D photonic crystal based biosensor for detection of cervical cancer cell. In: 2020 IEEE international conference on electronics, computing and communication technologies (CONECCT) (pp 1–4). IEEE

Kumar N, Suthar B (2019) Advances in photonic crystals and devices. CRC Press

Kurt H, Citrin DS (2005) New approaches in biochemical sensing using photonic crystals in the terahertz region. In: 2005 Joint 30th international conference on infrared and millimeter waves and 13th international conference on terahertz electronics (vol 1, pp 36–37). IEEE

Luff BJ, Harris RD, Wilkinson JS, Wilson R, Schiffrin DJ (1996) Integrated-optical directional coupler biosensor. Opt Lett 21(8):618–620

Nair RV, Vijaya R (2010) Photonic crystal sensors: an overview. Prog Quantum Electron 34(3):89–134

Naresh V, Lee N (2021) A review on biosensors and recent development of nanostructured materials-enabled biosensors. Sensors 21(4):1109

Nischita R, Gudagunti FD, Sharan P, Srinivas T (2015) 2-D photonic crystal based bio-chip for DNA analysis of breast cancer. In: 2015 International conference on pervasive computing (ICPC) (pp 1–4). IEEE

Olyaee S, Mohebzadeh-Bahabady A (2014) Two-curve-shaped biosensor using photonic crystal nano-ring resonators. J Nanostruct 4(3):303–308

Painam B, Kaler RS, Kumar M (2017) Photonic crystal waveguide biochemical sensor for the approximation of chemical components concentrations. Plasmonics 12(3):899–904

Painam B, Teotia P, Kaler RS, Kumar M (2014) Bio-chemical sensor based on photonic crystal waveguide for estimation of sulphuric acid concentration. In: International conference on fibre optics and photonics (pp S5A–48). Optical Society of America.

Painam B, Kaler RS, Kumar M (2016) Active layer identification of photonic crystal waveguide biosensor chip for the detection of Escherichia coli. Opt Eng 55(7):077105

Patil H, Ashwini M, Indumathi TS, Sharan P (2013) Design and analysis of photonic crystal based fluidic sensor. In: Fifth international conference on advances in recent technologies in communication and computing (ARTCom 2013) (pp 183–188). IET

Radhouene M, Balaji VR, Najjar M, Robinson S, Janyani V, Murugan M (2021) Rounded square ring resonator based add drop filter for WDM applications using two dimensional photonic crystals. Opt Quant Electron 53(5):1–24

Radhouene M, Chhipa MK, Najjar M, Robinson S, Suthar B (2017) Novel design of ring resonator based temperature sensor using photonics technology. Photon Sensors 7(4):311–316

Rajasekar R, Jayabarathan JK, Robinson S (2019) Nano-optical filter based on multicavity coupled photonic crystal ring resonator. Phys E: Low-Dimen Syst Nanostruct 114:113591

Rajasekar R, Robinson S (2018a) Nano-electric field sensor based on two dimensional photonic crystal resonator. Opt Mater 85:474–482

Rajasekar R, Robinson S (2018b) Trapezoid 2D photonic crystal nanoring resonator-based channel drop filter for WDM systems. Photon Netw Commun 36(2):230–245

Robinson S, Dhanlaksmi N (2017) Photonic crystal based biosensor for the detection of glucose concentration in urine. Photon Sensors 7(1):11–19

Robinson S, Nakkeeran R (2012a) Investigation on two dimensional photonic crystal resonant cavity based bandpass filter. Optik 123(5):451–457

Robinson S, Nakkeeran R (2012b) PC based optical salinity sensor for different temperatures. Photon Sensors 2(2):187–192

Salmanpour A, Mohammadnejad S, Bahrami A (2015) Photonic crystal logic gates: an overview. Opt Quant Electron 47(7):2249–2275

Sani MH, Ghanbari A, Saghaei H (2021) High-sensitivity biosensor for simultaneous detection of cancer and diabetes using photonic crystal microstructure. Opt Quant Electron. https://doi.org/10.21203/rs.3.rs-451630/v1

Sharma P, Sharan P (2014) An optical sensor for propagation analysis of Lymphocyte cell for cancer cell detection. In: 2014 IEEE global humanitarian technology conference-south asia satellite (GHTC-SAS) (pp 93–98). IEEE

Sharma P, Sharan P, Deshmukh P (2015) A photonic crystal sensor for analysis and detection of cancer cells. In: 2015 International conference on pervasive computing (ICPC) (pp 1–5). IEEE

Sharma P, Sharan P (2014a) Design of photonic crystal-based biosensor for detection of glucose concentration in urine. IEEE Sens J 15(2):1035–1042

Sharma P, Sharan P (2015) An analysis and design of photonic crystal-based biochip for detection of glycosuria. IEEE Sens J 15(10):5569–5575

Singh S, Kumar V, Dhanjal DS, Datta S, Prasad R, Singh J (2020) Biological biosensors for monitoring and diagnosis. In: Microbial biotechnology: basic research and applications (pp 317–335). Springer, Singapore

Suganya T, Robinson S (2017) 2D photonic crystal based biosensor using rhombic ring resonator for glucose monitoring. ICTACT Microelectron 3(1):349–353

Sundhar A, Valli R, Robinson S, Abinayaa A, SivaBharathy C (2019) Two dimensional photonic crystal based bio sensor for cancer cell detection. In: 2019 IEEE international conference on system, computation, automation and networking (ICSCAN) (pp 1–3). IEEE

Suzuki T, Yu PK (1999) Existence of photonic band gaps in two-dimensional metallodielectric photonic crystals. Electromagnetics 19(3):321–335. https://doi.org/10.1063/1.107868

Swain KP, Palai G (2016) Estimation of human-hemoglobin using honeycomb structure: an application of photonic crystal. Optik 127(6):3333–3336

Tameh TA, Isfahani BM, Granpayeh N, Javan AM (2011) Improving the performance of all-optical switching based on nonlinear photonic crystal microring resonators. AEU-Int J Electron Commun 65(4):281–287

Yablonovitch E (1987) Inhibited spontaneous emission in solid-state physics and electronics. Phys Rev Lett 58(20):2059